JOURNAL OF SOLID STATE CHEMISTRY 43, 196–203 (1982)

On the Defect Structure of Calcium Titanate with Nonideal Cationic Ratio

N. G. EROR AND U. BALACHANDRAN

Oregon Graduate Center, Beaverton, Oregon 97006

Received December 28, 1981

The defect structure of polycrystalline calcium titanate with Ca/Ti = 0.998, 0.995, and 0.992 was investigated by measuring the equilibrium electrical conductivity as a function of oxygen partial pressure ($P_{O_2} = 10^{0}$–10^{-20} atm) at 950–1050°C. These data were similar to that obtained in the sample with ideal cationic ratio. The deviation from ideal Ca-to-Ti ratio is found to be accommodated by the formation of neutral vacancy pairs, $(V_{Ca}'' V_{O}^{\cdot\cdot})$. The results indicate that the single-phase field of calcium titanate extends beyond 50.201 mole% TiO_2.

Introduction

Calcium titanate has an orthorhombic structure at room temperature (*1*), and the structure becomes tetragonal at ~600°C and cubic at ~1000°C (*2*). George and Grace (*3, 4*) examined the electrical conductivity, Seebeck coefficient, and diffusion of point defects in single-crystal $CaTiO_3$ in water–hydrogen atmospheres in the temperature range 1100–1300°C. Cox and Tredgold (*5*) measured the electrical conductivity of single-crystal $CaTiO_3$ at 130°C and reported it to be *p*-type, presumably after exposure to oxidizing atmospheres. Balachandran *et al.* (*6, 7*) studied the defect structure of undoped and lanthanum-added polycrystalline $CaTiO_3$. The reported studies on $CaTiO_3$ indicate that there is an extensive range of low oxygen partial pressures (P_{O_2}), where the conductivity increases with decreasing P_{O_2}, characteristic of *n*-type conduction related to oxygen deficiency.

The structural analog, $BaTiO_3$, has been studied in much detail in both polycrystalline (*8–13*) and single-crystal (*14*) states. The three polycrystalline samples of $BaTiO_3$ used by Long and Blumenthal (*10*) were found to be 2.1, 4.6, and 6.0 mole% deficient in BaO by chemical analysis. They noted no systematic variation of the equilibrium electrical conductivity among these samples. A comparison of the samples with an ideal cationic ratio and a 0.1 mole% deficiency in BaO showed no major differences in the electrical conductivity values (*13*). Recently, Chan *et al.* (*15*) studied the defect chemistry of strontium titanate with different Sr-to-Ti ratios by means of the high-temperature electrical conductivity as a function of P_{O_2}. They concluded that $SrTiO_3$ saturates with TiO_2 at less than 50.1 mole% and the defects formed due to the deviation from ideal cationic ratio are unassociated. In disagreement with the above results, the present authors (*16*) have found that the single-phase field of strontium titanate ex-

0022-4596/82/080196-08$02.00/0

tends beyond 50.505 mole% TiO_2 and the defects formed due to excess TiO_2 are associated into neutral vacancy pairs, $(V_{\mathrm{Sr}}'' V_{\mathrm{O}}^{\cdot\cdot})$.

In the present study, the electrical conductivity in calcium titanate with different Ca-to-Ti ratios was measured at 950 and 1050°C while in equilibrium with the oxygen partial pressure of the surrounding atmosphere. The Ca-to-Ti ratios selected were 0.998, 0.995, and 0.992, which correspond to 50.05, 50.125, and 50.201 mole% TiO_2, respectively. The conductivity data obtained in a sample with ideal cation–cation ratio in our previous investigation (*6*) are also given.

Experimental

The specimens employed in this investigation were prepared by a liquid mix technique (*6, 17, 18*). The powder samples were pressed into thin circular disks at 40,000 psi and sintered in air at 1350°C for 12 hr. Electrical conductivity specimens were cut from the sintered disks using an airbrasive unit. The specimens were wrapped with four 0.025-cm platinum wires as described in the literature (*19, 20*). Small notches were cut in the edges of the sample to aid in holding the platinum wires in place. A conventional four-probe direct current technique was employed for all electrical conductivity measurements and the experimental details have been described previously (*17*).

Results and Discussion

The measured electrical conductivity as a function of oxygen partial pressure in cal-

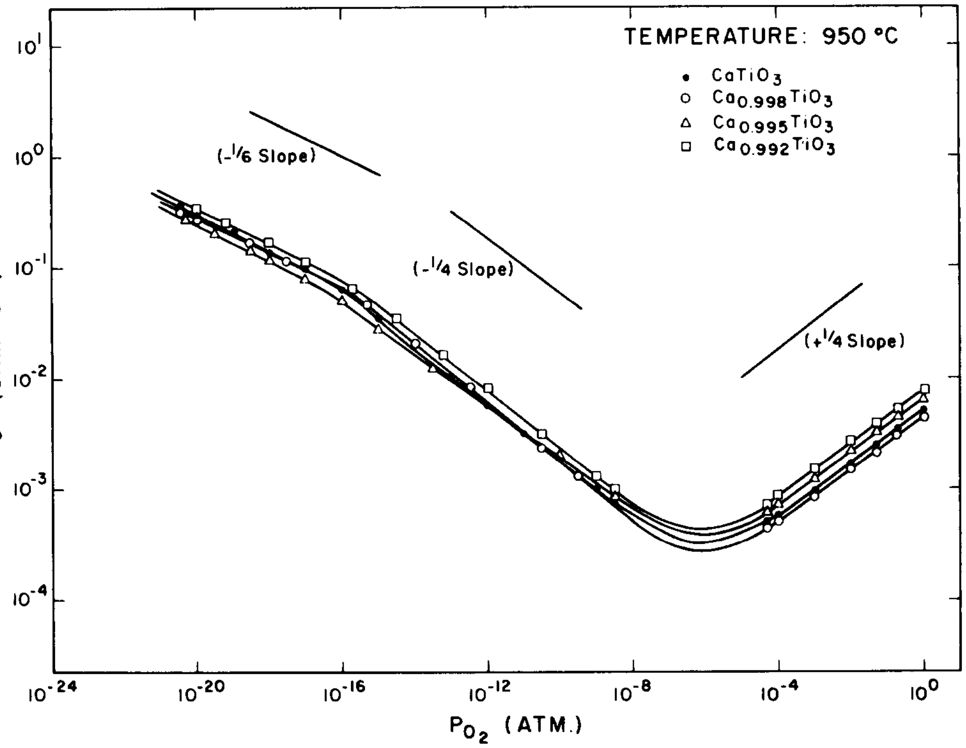

FIG. 1. The measured electrical conductivity as a function of P_{O_2} in calcium titanate with Ca/Ti = 1.000, 0.998, 0.995, and 0.992 at 950°C.

cium titanate with Ca/Ti = 1.000, 0.998, 0.995, and 0.992 at 950 and 1050°C are given in Figs. 1 and 2. In all the cases, the electrical conductivity changes from *p*- to *n*-type as the oxygen partial pressure is decreased. The log σ vs log P_{O_2} data are linear with a slope of $\sim -\frac{1}{6}$ in the P_{O_2} region $< 10^{-16}$ atm for all the samples investigated. As the oxygen activity is increased further, the P_{O_2} dependence of conductivity changes and the new values of the slopes are $\sim -\frac{1}{4}$ for the P_{O_2} range 10^{-15}–10^{-8} atm.

For $P_{O_2} > 10^{-4}$ atm, the conductivity increases with oxygen pressure, characteristic of *p*-type or oxygen excess conduction. The region of linearity in the *p*-type region increases in width with decreasing temperature (from 1050 to 950°C) as the *p*–*n* transition moves to lower P_{O_2}. The conductivity minima occur almost at the same P_{O_2} for all the samples. This is in disagreement with the prediction of Chan *et al.* (*15*) in $SrTiO_3$ that the conductivity minima move to lower P_{O_2} by two orders of magnitude for each order of magnitude increase in the extrinsic $V_O^{\cdot\cdot}$ concentration present as unassociated defect in the samples with excess TiO_2. The three regions observed in the log σ vs log P_{O_2} plots are discussed separately.

Region I ($P_{O_2} < 10^{-16}$ *atm*)

The slopes observed ($\sim -\frac{1}{6}$) for the log σ vs log P_{O_2} plots in this region are similar to that found for $BaTiO_3$ (*11–14*) and $SrTiO_3$ (*16, 17*) as well as the results obtained in polycrystalline calcium titanate with Ca/Ti = 1.000 (*6*). Excess TiO_2 in the system must be accommodated by the formation of point defects in the lattice. The following mechanisms can be envisioned for the in-

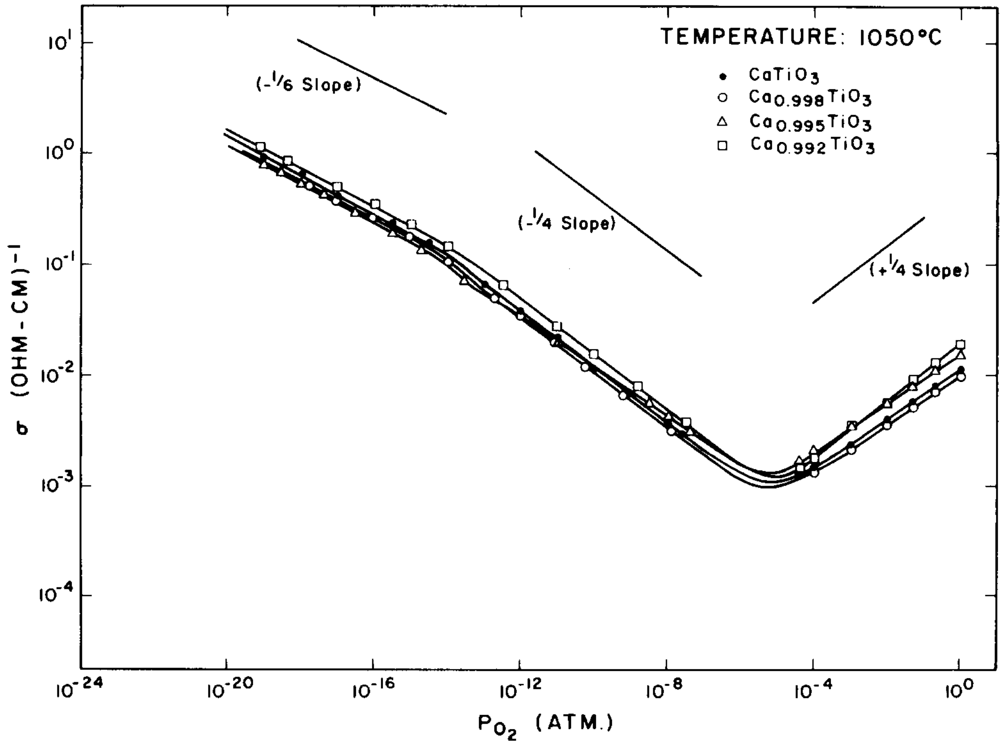

FIG. 2. The measured electrical conductivity as a function of P_{O_2} in calcium titanate with Ca/Ti = 1.000, 0.998, 0.995, and 0.992 at 1050°C.

corporation of excess TiO_2 into $CaTiO_3$ of ideal composition to make Ca-to-Ti ratio less than unity:

$$TiO_2 \rightleftharpoons Ti_i^{4+} + 2O_i^{2-}, \quad (1)$$

$$TiO_2 \rightleftharpoons Ti_i^{4+} + O_2 + 4e', \quad (2)$$

$$2TiO_2 \rightleftharpoons Ti_{Ca}^{2+} + Ti_{Ti}^{x} + 3O_O^x + O_i^{2-}, \quad (3)$$

$$2TiO_2 \rightleftharpoons Ti_{Ca}^{2+} + Ti_{Ti}^{x} + 3O_O^x + 2e' + \tfrac{1}{2}O_2, \quad (4)$$

$$TiO_2 \rightleftharpoons Ti_{Ti}^{x} + 2O_O^x + V_{Ca}'' + V_O^{\cdot\cdot}, \quad (5)$$

$$TiO_2 + \tfrac{1}{2}O_2 \rightleftharpoons Ti_{Ti}^{x} + 3O_O^x + V_{Ca}'' + 2h. \quad (6)$$

The reactions [Eqs. (2), (4), and (6)] which generate electronic defects can be excluded because of the observed lack of influence of the Ca/Ti ratio on the electronic conductivity (Figs. 1 and 2). Both Ti_i^{4+} and O_i^{2-} are unfavorable defects in the close-packed perovskite structure, so Eq. (5), involving the formation of (V_{Ca}'' and $V_O^{\cdot\cdot}$), is the most probable choice. This is in accord with the electrical conductivity measurements in $CaTiO_3$ (*3, 6*) which showed that $V_O^{\cdot\cdot}$ is the preferred defect for oxygen deficiency in $CaTiO_3$, and they appear to be the dominant ionic defect in the closely related $BaTiO_3$ (*10, 11, 14*) and $SrTiO_3$ (*15, 17*) in the oxygen-deficient region.

The chemical mass action expression for reaction (5) is given by

$$[V_{Ca}''][V_O^{\cdot\cdot}] \approx K_5 a_{TiO_2}, \quad (7)$$

where a_{TiO_2} is the activity of TiO_2. One should also consider the formation of a doubly ionized oxygen vacancy, $[V_O^{\cdot\cdot}]$, and two electrons available for conduction by the removal of an oxygen from a normal lattice site into the gas phase in TiO_2-excess $CaTiO_3$. The reaction is

$$O_O^x \rightleftharpoons \tfrac{1}{2}O_2 + V_O^{\cdot\cdot} + 2e'. \quad (8)$$

The equilibrium constant for reaction (8) is

$$K_8 \approx [V_O^{\cdot\cdot}][n]^2 P_{O_2}^{1/2} \approx \exp\left(\frac{-\Delta G_f}{RT}\right), \quad (9)$$

where $[n] \equiv e'$. The Gibbs standard free energy change for reaction (8) is represented by ΔG_f. If the built-in CaO deficiency exceeds the disorder from the oxygen loss described in Eq. (8), the charge neutrality condition will then read

$$[V_{Ca}''] \approx [V_O^{\cdot\cdot}] \approx K_5^{1/2} a_{TiO_2}^{1/2}. \quad (10)$$

From Eqs. (9) and (10) we can then obtain

$$[n] = \left[\frac{K_8^{1/2}}{K_5^{1/4} a_{TiO_2}^{1/4}}\right] P_{O_2}^{-1/4}. \quad (11)$$

The data in Figs. 1 and 2 indicate that in the P_{O_2} region $<10^{-16}$ atm the conductivity varies as $P_{O_2}^{-1/6}$. This indicates that at low P_{O_2} the charge neutrality condition should be

$$[n] \approx 2[V_O^{\cdot\cdot}]. \quad (12)$$

Expressing the free energy change in terms of the enthalpy change, ΔH_f, and entropy change, ΔS_f, and substituting Eq. (12) into Eq. (9), the result for the electron concentration is

$$[n] = 2^{1/3} P_{O_2}^{-1/6} \exp\left[\frac{\Delta S_f}{3R}\right] \exp\left[\frac{-\Delta H_f}{3RT}\right] \quad (13)$$

and the electrical conductivity, σ, is given by

$$\sigma = 2^{1/3} P_{O_2}^{-1/6} e\,\mu \exp\left[\frac{\Delta S_f}{3R}\right] \exp\left[\frac{-\Delta H_f}{3RT}\right], \quad (14)$$

where e is the electronic charge and μ is the mobility of the conduction electrons. For Eq. (12) to hold, the oxygen deficiency created by Eq. (8) must greatly exceed the built-in CaO deficiency.

Thermogravimetric measurements on undoped $CaTiO_3$ (*21*) indicate that for Eq. (12) to be a valid expression for the dominant charged defects, no other charged defect can be present in excess of about 450 ppm (atomic). For the samples under consideration, the CaO deficiency amounts to 2000–8000 ppm. From the known amounts of CaO deficiency in the samples, the observed $-\frac{1}{6}$th dependence for conductivity on P_{O_2} is possible only when the defects related to CaO deficiency are associated into neutral complexes, such as vacancy pairs, to such an extent that the residual, isolated, charged defects from this source do not affect the condition of charge neutrality, Eq. (12), and thus have no influence on the oxygen-deficient defect chemistry. Otherwise, reaction (8) could not become the dominant source of $[V_O^{\cdot\cdot}]$ at low oxygen pressures and the relationship $\sigma \propto P_{O_2}^{-1/6}$ would not be observed. If the defects formed due to the CaO deficiency are unassociated, then the measured conductivity should change significantly as the Ca-to-Ti ratios are changed. There is no significant change in conductivity between the samples with different Ca-to-Ti ratios (see Figs. 1 and 2). The association reaction can be represented as

$$V''_{Ca} + V_O^{\cdot\cdot} \rightleftharpoons (V''_{Ca} V_O^{\cdot\cdot}), \tag{15}$$

where the parentheses indicate that the enclosed species are electrostatically bound to adjacent lattice sites. It has been reported in the literature (*13, 14*) that the defects formed due to excess TiO_2 in $BaTiO_3$ are associated into neutral vacancy pairs $(V''_{Ba} V_O^{\cdot\cdot})$.

The phase information available to date for the $CaO–TiO_2$ system (*22*) shows that there is a definite phase width for $CaTiO_3$ on the CaO-rich side and a single-phase region from the ideal composition of $CaTiO_3$ up to ~2–3 mole% excess CaO at 1200°C, but no indication of any solubility for excess TiO_2 in $CaTiO_3$. The phase diagram for the structural analog $BaO–TiO_2$ shows that there is a definite phase width (~1 mole% excess TiO_2) on the TiO_2-rich side of $BaTiO_3$ at 1400°C (*23*). In disagreement with the above results, Sharma *et al.* (*24*) reported that the solubility of TiO_2 in $BaTiO_3$ is less than 0.1 mole%. The available phase study in the system $CaO–TiO_2$ (*22*) suggests that the second phase formed for excess TiO_2 in $CaTiO_3$ should be TiO_2. The presence of second phase in the polycrystalline samples should have some effect on transport properties, such as electrical conductivity or oxygen self-diffusion. In the electrical conductivity studies of samples with Ca/Ti = 0.998, 0.995, and 0.992, equilibrium was established as fast as it was obtained in the sample with ideal cationic ratio. Also, in the sample with 50.201 mole% TiO_2 (Ca/Ti = 0.992) no second phase was observed optically or by X-ray diffraction technique. This indicates that for the conditions under which the present samples are sintered, the $CaTiO_3$ does not saturate with TiO_2 even at 50.201 mole%. This suggests that $BaTiO_3$ (*22*), $SrTiO_3$ (*15, 16*), and $CaTiO_3$ all have a definite phase width on the TiO_2-rich side of the phase diagram. The actual width of the phase boundary, however, may be different in each of these alkaline earth titanates.

Region II ($P_{O_2} = 10^{-15}$–10^{-8} *atm*)

A slope of ~$-\frac{1}{4}$ is found for the log σ vs log P_{O_2} data (see Figs. 1 and 2). Balachandran *et al.* (*6*) attributed the observed slope of approximately $-\frac{1}{4}$ in the sample with Ca/Ti = 1.000 to the presence of small amounts of unknown acceptor impurities in the undoped samples. For the case of undoped $SrTiO_3$ prepared by the same technique as that used here, the present authors (*17*) have estimated an unknown acceptor impurity concentration of about 170 ppm. Potential acceptor elements are naturally much more abundant than potential donor elements. We believe that the present samples also contain some unknown acceptor impurities.

In order to discuss the concept of the impurity effect, it is helpful to consider a Kröger–Vink (*25*) diagram for a ternary oxide of the type ABO_3 with an acceptor impu-

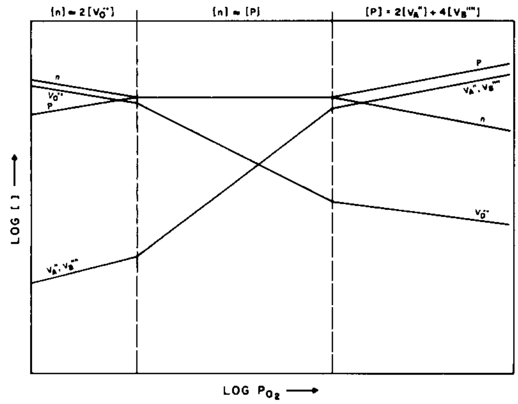

FIG. 3. Defect concentration vs the oxygen pressure in the ternary oxide ABO_3 with Schottky–Wagner disorder.

rity. We will, for the purpose of illustration, consider Schottky–Wagner disorder to describe the nonstoichiometry. Figure 3 illustrates the variation of defect concentrations as a function of oxygen partial pressure for the case of fully ionized atomic defects, electrons, $[n]$, and electron holes, $[p]$, in pure ABO_3 with both A and B site vacancies. The familiar $[n] \propto P_{O_2}^{-1/6}$ region with charge neutrality condition, $[n] \approx 2\,[V_O^{\cdot\cdot}]$, is illustrated in Fig. 3. In Fig. 4, an acceptor impurity I_m that is always fully ionized to I_m' is added to the ternary oxide ABO_3. Note in Fig. 4 that for sufficient departures from stoichiometry it may be possible for the electrical conductivity to be controlled by $[n] \approx 2[V_O^{\cdot\cdot}]$ and to thereby mask the effect of the acceptor impurity.

In Fig. 4, there is a region with electrical neutrality condition, $[I_m'] \approx 2\,[V_O^{\cdot\cdot}]$, in which the electron concentration varies as the $-\frac{1}{4}$th power and the electron hole concentration increases as the $+\frac{1}{4}$th power of oxygen partial pressure. In this region, for certain values of P_{O_2}, the electron concentration is greater than the electron hole concentration and, hence, the conductivity is n-type with a $-\frac{1}{4}$th dependence on P_{O_2}. As the oxygen partial pressure increases, the electron hole concentration eventually becomes greater than the electron concentration and the material becomes p-type with a $+\frac{1}{4}$th dependence for conductivity on P_{O_2}. When the P_{O_2} value is increased further, the electron hole concentration becomes equal to the acceptor concentration, which is constant, and hence the conductivity is independent of P_{O_2}, with the charge neutrality condition, $[I_m'] \approx [p]$, as shown in Fig. 4.

The observed slope of $\sim -\frac{1}{4}$ from the log σ vs log P_{O_2} data (see Figs. 1 and 2) in this region of P_{O_2} (10^{-15}–10^{-8} atm) is interpreted in terms of the presence of accidental acceptor impurities, such as Fe, Al, or Cr on Ti sites. The condition of charge neutrality in this region is

$$[I_m'] \approx 2\,[V_O^{\cdot\cdot}]. \tag{16}$$

With this neutrality condition and Eqs. (8) and (9), the electrical conductivity varies with oxygen partial pressure as shown in

$$\sigma = 2^{1/2}\frac{1}{[I_m']^{1/2}}P_{O_2}^{-1/4}e\,\mu \\ \exp\left[\frac{\Delta S_f}{2R}\right]\exp\left[\frac{-\Delta H_f}{2RT}\right]. \tag{17}$$

The observed P_{O_2} dependence of conductivity in all the samples are in good agreement

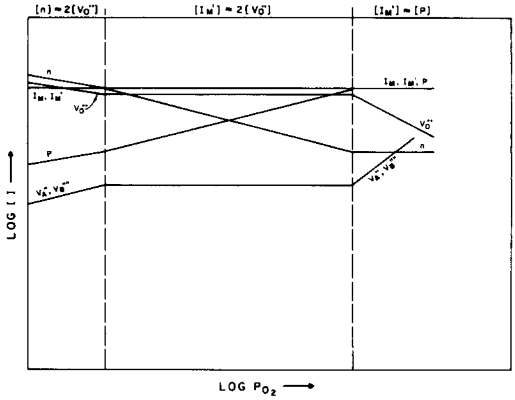

FIG. 4. Defect concentration for the ternary oxide ABO_3 with a fully ionized acceptor impurity, I_m', and Schottky–Wagner disorder as a function of oxygen pressure.

with the value predicted by the above impurity model.

Region III ($P_{O_2} > 10^{-4}$ *atm*)

The electrical conductivity in this region is *p*-type with a $\sim+\frac{1}{4}$th dependence on P_{O_2}. The *p*-type behavior is due to the incorporation of oxygen atoms into the calcium titanate lattice. Stoichiometric excess of oxygen (more than enough oxygen to satisfy the maximum oxidation states of the cationic content) can be incorporated into calcium titanate by a favorable process (*6, 14, 17*). The CaO deficiency makes available systematic oxygen vacancies which might accommodate a stoichiometric excess of oxygen according to

$$(V''_{Ca}V_O^{\cdot\cdot}) + \tfrac{1}{2}O_2 \rightleftharpoons O_O^x + V'_{Ca} + h^{\cdot}, \quad (18)$$

$$\frac{[V'_{Ca}][p]}{[(V''_{Ca}V_O^{\cdot\cdot})]} = K_{18}P_{O_2}^{1/2} = K_{19}P_{O_2}^{1/2}\exp\left[\frac{-\Delta H_p}{RT}\right], \quad (19)$$

where $[p] \equiv h^{\cdot}$. $[(V''_{Ca}V_O^{\cdot\cdot})]$ can be taken as constant in Eq. (19) for a given composition. The unassociated calcium vacancies that result when the oxygen vacancy in the neutral calcium vacancy–oxygen vacancy complex is filled must be singly ionized in order to lead to the $+\frac{1}{4}$ oxygen partial pressure dependence of the electrical conductivity data when Eq. (19) is combined with the corresponding charge neutrality condition,

$$[V'_{Ca}] \approx [p]. \quad (20)$$

The combination of Eqs. (19) and (20), however, indicates that $[p]$ and, therefore, the conductivity in this region should be proportional to $[(V''_{Ca}V_O^{\cdot\cdot})]^{1/2}$. No such variation in the electrical conductivity was observed (Figs. 1 and 2), which suggests that the bound $V_O^{\cdot\cdot}$ related to the CaO deficiency does not offer the sites for the incorporation of oxygen atoms to lead to the observed *p*-type behavior. It is to be pointed out here that Chan and Smyth (*13*) compared barium titanate samples with Ba-to-Ti ratios of 0.995 and 1.000 whereby the concentration of the divacancy complex should have differed by at least two orders of magnitude and found that the conductivity for the latter samples was higher by only about 30%, which is even in the wrong direction according to the above model (*14*). If one assumes that the defects formed due to the CaO deficiency are unassociated, then one would expect the conductivity in the *p*-type region to increase as the CaO deficiency increases. This is because a greater number of oxygen atoms can be incorporated into the oxygen vacancies from the unassociated defects. No such systematic variation in the absolute values of the conductivity was observed (see Figs. 1 and 2) for the wide range of CaO deficiency introduced into the samples used in the present study.

The observed *p*-type behavior, therefore, is due to the incorporation of oxygen into the impurity-related oxygen vacancies and the reaction is

$$[V_O^{\cdot\cdot}] + \tfrac{1}{2}O_2 \rightleftharpoons O_O^x + 2h^{\cdot} \quad (21)$$

The charge neutrality condition in this region is given by

$$[I'_m] \approx 2[V_O^{\cdot\cdot}]. \quad (16)$$

The chemical mass action expression for Eq. (21) is

$$\frac{[p]^2}{[V_O^{\cdot\cdot}]} = K_{21}P_{O_2}^{1/2} = K'_{21}P_{O_2}^{1/2}\exp\left[\frac{-\Delta H_p}{RT}\right] \quad (22)$$

Combination of Eqs. (16) and (22) gives

$$[p] = \left(\frac{K'_{21}[I'_m]}{2}\right)^{1/2} P_{O_2}^{1/4}\exp\left(\frac{-\Delta H_p}{2RT}\right). \quad (23)$$

This yields

$$\sigma \propto P_{O_2}^{1/4} \quad (24)$$

as long as only a minor fraction of the impurity-related $V_O^{\cdot\cdot}$ is filled. This model fits the observed oxygen pressure dependence of electrical conductivity in this region.

Conclusions

The oxygen pressure dependence of electrical conductivity in the samples with Ca-to-Ti ratios 0.998, 0.995, and 0.992 (corresponds to 50.05, 50.125, and 50.201 mole% TiO_2, respectively) was found to be similar to that observed in calcium titanate with ideal cation–cation ratio. The absolute values of the conductivity did not change significantly as the Ca/Ti ratio was changed in all the three regions. These observations indicate that the defects related to the deviation from ideal cationic ratio are associated into neutral vacancy pairs, $(V''_{\text{Ca}} V_{\text{O}}^{\cdot\cdot})$, and this conclusion is similar to that obtained for the structural analogs $BaTiO_3$ and $SrTiO_3$ with excess TiO_2 by earlier investigators (*13, 14, 16*). The experimental results indicate that doubly ionized oxygen vacancies, Eq. (8), are the dominant defect present for $P_{O_2} < 10^{-16}$ atm.

For $P_{O_2} > 10^{-15}$ atm, the defect chemistry of calcium titanate is dominated by accidental acceptor impurities and their related oxygen vacancies, Eq. (16). Because of these acceptor impurities, a region in which the conductivity changes as the $\sim -\frac{1}{4}$th power of oxygen partial pressure is observed.

The *p*-type conductivity observed in the region $P_{O_2} > 10$ atm is due to fractional filling of the impurity-related oxygen vacancies, Eq. (21), and the defects present due to the deviation from ideal cationic ratio have no significant role in influencing the observed electrical conductivity. The conductivity minima occur almost at the same P_{O_2} for the samples with different Ca-to-Ti ratios. The results indicate that for the conditions under which the present samples were sintered, $CaTiO_3$ does not saturate with TiO_2 even at 50.201 mole%. The effect on the defect chemistry of $CaTiO_3$ with excess CaO is currently under investigation.

Acknowledgment

We wish to thank the Gas Research Institute for the financial support in carrying out this investigation.

References

1. H. F. Kay and P. C. Bailey, *Acta Crystallogr.* **10,** 219 (1957).
2. H. F. Kay, Rept. Brit. Elec. Res. Assoc. Ref. LT, 257 (1951).
3. W. L. George and R. E. Grace, *J. Phys. Chem. Solids* **30,** 881 (1969).
4. W. L. George and R. E. Grace, *J. Phys. Chem. Solids* **30,** 889 (1969).
5. G. A. Cox and R. H. Tredgold, *Brit. J. Appl. Phys.* **18,** 37 (1967).
6. U. Balachandran, B. Odekirk, and N. G. Eror, *J. Solid State Chem.* **41,** 185 (1982).
7. U. Balachandran, and N. G. Eror, Submitted.
8. H. Veith, *Z. Angew. Phys.* **20,** 16 (1965).
9. F. Fosek and H. Arend, *Phys. Status Solidi* **24,** K69 (1967).
10. S. A. Long and R. N. Blumenthal, *J. Amer. Ceram. Soc.* **54,** 515 (1971).
11. S. A. Long and R. N. Blumenthal, *J. Amer. Ceram. Soc.* **54,** 577 (1971).
12. A. M. J. H. Seuter, *Philips Res. Rep.,* Suppl. No. 3 (1974).
13. N. H. Chan and D. M. Smyth, *J. Electrochem. Soc.* **123,** 1584 (1976).
14. N. G. Eror and D. M. Smyth, *J. Solid State Chem.* **24,** 235 (1978).
15. N. H. Chan, R. K. Sharma, and D. M. Smyth, *J. Electrochem. Soc.* **128,** 1762 (1981).
16. N. G. Eror and U. Balachandran, *J. Solid State Chem.,* in press.
17. U. Balachandran and N. G. Eror, *J. Solid State Chem.* **39,** 351 (1981).
18. M. Pechini, U.S. Patent 3,330,697, July 11, 1967.
19. S. P. Mitoff, *J. Chem. Phys.* **35,** 882 (1961).
20. J. B. Price and J. B. Wagner, *Z. Phys. Chem.* **49,** 257 (1966).
21. U. Balachandran and N. G. Eror, *J. Mater. Sci.* **17,** No. 5 (1982).
22. R. C. DeVries, R. Roy, and E. F. Osborn, *J. Phys. Chem.* **58,** 1069 (1954).
23. D. E. Rase and R. Roy, *J. Amer. Ceram. Soc.* **38,** 102 (1955).
24. R. K. Sharma, N. H. Chan, and D. M. Smyth, *J. Amer. Ceram. Soc.* **64,** 448 (1981).
25. F. A. Kröger and J. H. Vink, *in* "Solid State Physics" (F. Seitz and D. Turnbull, Eds.), Vol. 3, p. 307, Academic Press, New York (1956).